# Entry of Cell-Penetrating Peptide Transportan 10 into a Single Vesicle by Translocating Across Lipid Membrane and Its Induced Pores

BIOCHEMISTRY
including biophysical chemistry & molecular biology

Article

pubs.acs.org/biochemistry

# Entry of Cell-Penetrating Peptide Transportan 10 into a Single Vesicle by Translocating Across Lipid Membrane and Its Induced Pores

Md. Zahidul Islam,[†] Hirotaka Ariyama,[†] Jahangir Md. Alam,[‡] and Masahito Yamazaki*[,†,‡,§]

[†]Integrated Bioscience Section, Graduate School of Science and Technology, [‡]Nanomaterials Research Division, Research Institute of Electronics, and [§]Department of Physics, Graduate School of Science, Shizuoka University, Shizuoka 422-8529, Japan

**ABSTRACT:** The cell-penetrating peptide, transportan 10 (TP10), can translocate across the plasma membrane of living cells and thus can be used for the intracellular delivery of biological cargo such as proteins. However, the mechanisms underlying its translocation and the delivery of large cargo remain unclear. In this report we investigated the entry of TP10 into a single giant unilamellar vesicle (GUV) and the TP10-induced leakage of fluorescent probes using the single GUV method. GUVs of 20% dioleoylphosphatidylglycerol (DOPG)/80% dioleoylphosphatidylcholine (DOPC) were prepared, and they contained a water-soluble fluorescent dye, Alexa Fluor 647 hydrazide (AF647), and smaller vesicles composed of 20% DOPG/80% DOPC. The interaction of carboxyfluorescein (CF)-labeled TP10 (CF-TP10) with these loaded GUVs was investigated using confocal microscopy. The fluorescence intensity of the GUV membrane increased with time to a saturated value, then the fluorescence intensity due to the membranes of the smaller vesicles inside the GUV increased prior to leakage of AF647. This result indicates that CF-TP10 entered the GUV from the outside by translocating across the lipid membrane before CF-TP10-induced pore formation. The rate constant of TP10-induced pore formation in lipid membranes increased with an increase in TP10 concentration. Large molecules such as Texas Red Dextran 40 000, and vesicles with a diameter of 1−2 $\mu$m, permeated through the TP10-induced pores or local rupture in the lipid membrane. These results provide the first direct experimental evidence that TP10 can deliver large cargo through lipid membranes, without the need for special transport mechanisms such as those found in cells.

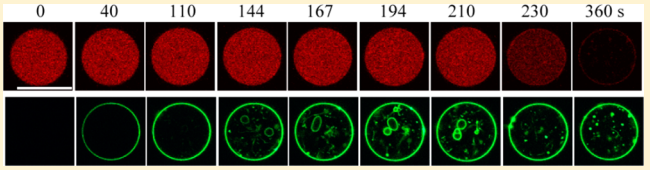


Cell-penetrating peptides (CPPs) can translocate across the plasma membrane of living cells and thus can be used for the intracellular delivery of biological cargo such as proteins and oligonucleotides.[1−5] CPPs can be classified into two groups based on their physicochemical characteristics: amphipathic and nonamphipathic CPPs. Penetratin, pVEC, transportan (TP), and TP10, a truncated analogue of TP, are amphipathic CPPs. TAT and R9 contain many Arg residues and are nonamphipathic CPPs. The mechanism by which CPPs and their cargo translocate across the plasma membrane is still controversial. Some CPPs internalize via endocytosis, but others use nonendocytosis pathways.[1−5] In both cases, CPPs must translocate across the lipid bilayer to enter a cell.

TP, a synthetic CPP, consists of a neuropeptide, galanin, at the N-terminus and a wasp venom peptide, mastoparan, at the C-terminus. TP can translocate across the plasma membrane of cells by a receptor-independent mechanism.[6,7] To reduce the inhibitory effect of TP on GTPase activity, a truncated analogue, TP10, has been synthesized by the deletion of six amino acids from the N-terminus of TP. TP10 has cell-penetrating activity.[8,9] As TP10 does not bind to galanin receptors, its likely target is the lipid bilayer of the plasma membrane. TP10 is probably internalized by nonendocytosis pathways, since various endocytosis inhibitors have no effect on its translocation.[8] TP and TP10 can deliver a large protein such as an antibody, oligonucleotide, and colloidal gold (diameter 10 nm) as cargo.[7,9]

The interaction of TP10 with lipid membranes has been investigated using a suspension of small liposomes (LUVs) (the LUV suspension method[10−12]). TP10 induced gradual leakage (diffusion) of a small water-soluble fluorescent probe, carboxyfluorescein, from the inside to the outside of LUVs in a concentration-dependent manner.[10] Results from fluorescence ANTS/DPX assays suggested that the leakage of fluorescent probes is "graded". The data were analyzed assuming that the leakage of these fluorescent probes occurs during the translocation of TP10 across the lipid bilayer.[10,11] This state was defined as the TP10-induced pore in the lipid membrane. However, in the LUV suspension method, the average values of the physical parameters of the liposomes are obtained from a large number of liposomes which are in different elementary steps of the peptide-induced structural change, and therefore much information is lost.[13,20] Moreover, the LUV suspension method does not allow determination of the main cause of leakage because many factors could be involved, such as pore formation, membrane fusion, rupture, and fragmentation of liposomes. These structural changes

**Received:** October 14, 2013
**Revised:** December 30, 2013
**Published:** January 3, 2014

  

cannot be directly detected in LUVs in suspension. It is therefore difficult to identify the mechanism of translocation of TP10 across the lipid membrane, and the mechanism of TP10-induced leakage of fluorescent probes, using only the LUV suspension method.

Recently, giant liposomes or giant unilamellar vesicles (GUVs) with diameters greater than 10 $\mu$m have been used to investigate the physical properties of vesicle membranes, such as shape change and phase separation.[14,15] The shape of a single GUV and its physical properties in water can be measured in real time. Based on the characteristics of these GUVs, we have developed a single GUV method to investigate the functions and dynamics of biomembranes.[13,16−21] Using this method, changes in the structure and physical properties of a single GUV induced by interactions with materials such as peptides and proteins are observed as a function of time and spatial coordinates. Then, the same experiments are repeated many times using other single GUV. The results are used to analyze statistically the changes in the physical properties of a single GUV to obtain rate constants of elementary processes for reactions of GUVs. For example, we studied peptide/protein-induced leakage (i.e., membrane permeation) of the internal contents (such as water-soluble fluorescent probes) from single GUVs using the single GUV method. This enabled identification of the cause of leakage and calculation of the rate constants of elementary processes involved in leakage (such as peptide/protein-induced pore formation in lipid membranes, and leakage of fluorescent probes through the pores).[13] We have determined the rate constants of pore formation in lipid membranes induced by the antimicrobial peptide magainin 2 and the pore-forming toxin lysenin, and also the rate constant of membrane permeation of various fluorescent probes through these pores. These results have provided valuable information revealing the mechanisms of pore formation.[16−19]

In the present study, we used the single GUV method to investigate the translocation of TP10 across a lipid membrane into a GUV, and TP10-induced leakage of a water-soluble fluorescent probe from the inside to the outside of a GUV. Specifically, we investigated the translocation of a fluorescent probe, carboxyfluorescein (CF)-labeled TP10 (CF-TP10), across the lipid membrane and the leakage of a water-soluble fluorescein probe, Alexa Fluor 647 hydrazide (AF647), from 20% dioleoylphosphatidylglycerol (DOPG)/80% dioleoylphosphatidylcholine (DOPC)-GUVs simultaneously using confocal laser scanning microscopy (CLSM). To elucidate the translocation of TP10 with cargo molecules, we also investigated the permeation of larger molecules such as the fluorescent probe, Texas Red (TR)-labeled Dextran 40K (TRD-40k),[18] and lipid vesicles through the membranes. In addition, TP 10-induced structural changes of GUVs were studied. Based on the results, we discuss the fundamental steps by which TP10 translocates the lipid membrane and induces pore formation.

## MATERIALS AND METHODS

DOPC and DOPG were purchased from Avanti Polar Lipids Inc. (Alabaster, AL). Bovine serum albumin (BSA) was purchased from Wako Pure Chemical Industry Ltd. (Osaka, Japan). AF647, TRD-10k, TRD-40k, and N-((6-(biotinoyl)-amino)-hexanoyl)-1,2-dihexadecanoyl-*sn*-glycero-3-phosphoethanolamine, triethyl ammonium salt (biotin-X-DHPE, referred to as biotin-lipid) were purchased from Invitrogen Inc. (Carlsbad, CA). Calcein was purchased from Dojindo Laboratory (Kumamoto, Japan). Biotin-labeled BSA and streptavidin were purchased from Sigma-Aldrich Co. (St. Louis, MO, USA). TP10 was synthesized by the FastMoc method using a 433A peptide synthesizer (PE Applied Biosystems, Foster City, CA). The sequence of TP10 (21-mer) is AGYLLGKINLKALAALAKKIL and has an amide-blocked C terminus. The fluorescence probe carboxyfluorescein-labeled TP10 (CF-TP10), which has one fluorophore CF at the N-terminus of the peptide, was synthesized using a standard method[22] by the reaction of 5-(and 6)-carboxyfluorescein succinimidyl ester (Invitrogen) (19 mg) with TP10-peptide resin (80 mg) (molar ratio of reagent to peptide: 2.5 to1) in dimethylformamide for 24 h at room temperature. TP10 and CF-TP10 were cleaved from the resin using trifluoroacetic acid, 1,2-ethanedithiol, and Milli-Q water (9.5/0.25/0.25, volume ratio). The methods for purification and identification of these peptides were described previously.[16−18] The purified peptides were analyzed by ion-spray ionization mass spectrometry using a single quadrupole mass spectrometer (API 150*EX*, *PE SCIEX*, PE Applied Biosystems). The measured mass of TP10 and CF-TP10 was 2181 ± 1 Da and 2540 ± 1 Da, respectively, which correspond to the molecular mass calculated from the amino acid composition.

GUVs of DOPG/DOPC/biotin-lipid (molar ratio: 20/79/1, referred to as 20%DOPG/79%DOPC/1%biotin-lipid) were prepared by incubation of buffer H (10 mM HEPES, pH 7.5, 150 mM NaCl, and 1 mM EGTA) containing 0.1 M sucrose and various fluorescent probes with dry lipid films by the natural swelling at 37 °C.[16−18] The concentrations of the fluorescent probes were: 6 $\mu$M for AF647, 10 $\mu$M for TRD-10k, 10 $\mu$M for TRD-40k, and 1 mM calcein. To prepare GUVs containing smaller vesicles, a GUV suspension was prepared in a buffer containing no fluorescent probes using the above method, then the GUV suspension was centrifuged at 14 000 × *g* for 20 min at 20 °C to remove multilamellar vesicles and lipid aggregates. A mixture of the partially purified GUV suspension and AF647 solution in buffer H containing 0.1 M sucrose was incubated with dry lipid films at 37 °C. The membrane filtering method was used to remove untrapped fluorescent probes.[23]

Purified GUV suspension (300 $\mu$L: 0.1 M sucrose in buffer H as the internal solution; 0.1 M glucose in buffer H as the external solution) was transferred into a handmade microchamber.[13,16] Single GUVs were fixed on a slide glass or a coverslip in the chamber using the strong association between biotin and streptavidin, previously used to fix LUVs onto glass surfaces.[24] First, 0.9 mg/mL BSA and 0.1 mg/mL biotin BSA in buffer H containing 0.1 M glucose were added to the chamber and incubated. Excess biotin BSA and BSA were removed by washing with the same buffer, leaving a BSA/biotin-BSA coating on the glass surface of the chamber. Next, 0.025 mg/mL streptavidin and 0.1 mg/mL BSA in the same buffer were added to the chamber and incubated, then removed using the same buffer. Finally, a suspension of GUVs containing biotin-lipid was transferred into the chamber. Due to the strong binding of streptavidin with both the biotin-BSA adsorbed on the glass surface and the biotin-lipid in the GUV membrane, the GUV was connected to the glass surface via a tether comprising a long hydrophilic segment of biotin-lipid.

The GUVs were observed using a CLSM (FV-1000, Olympus, Tokyo, Japan) or an inverted fluorescence phase contrast microscope (IX-70, Olympus) at 25 ± 1 °C using a stage thermocontrol system (Thermoplate, Tokai Hit, Shizuoka, Japan). For CLSM measurements, fluorescence

images of AF647 (excited by a laser at $\lambda$ = 633 nm) and of CF-TP10 (excited by a laser at $\lambda$ = 488 nm) were obtained using a 60× objective (UPLSAPO060X0, Olympus) (NA = 1.35). For measurements using IX-70, phase contrast and fluorescence images of GUVs were recorded using a high-sensitivity fluorescence camera (EM-CCD camera, C9100−12, Hamamatsu Photonics K.K., Hamamatsu, Japan) containing a hard disk. Three ND filters were used to decrease the intensity of the incident light to reduce photobleaching of fluorescent probes. The fluorescence intensity inside the GUVs was determined using an AquaCosmos (Hamamatsu Photonics K.K.) and the average intensity per GUV was estimated. During the interaction of peptides with a single GUV, various concentrations of CF-TP10 or TP10 in buffer H containing 0.1 M glucose were added continuously to the vicinity of the GUV through a 20-$\mu$m-diameter glass micropipet positioned by a micromanipulator. The distance between the GUV and the tip of the micropipet was 50−60 $\mu$m. The details of this method were described previously.[13,16−21]

Obtaining the time course of the fluorescence intensity required special methodology because the GUVs were not fixed at one position, but rather moved slightly (less than 10 $\mu$m) during interaction with CF-TP10 (or TP10). To measure the time course of the fluorescence intensity of AF647 inside a GUV, we specified a larger region encompassing the entire area occupied by the GUV during the interaction of CF-TP10 (or TP10) and measured the fluorescence intensity of this area as a function of time. To measure the time course of the CF-TP10 fluorescence intensity at the rim of the GUV (i.e., the GUV membrane), a vertical line was drawn through the center of each GUV (Figure 1A) and the fluorescence intensity profile along the line was measured (Figure 1B). The two points with the highest intensity correspond to the GUV membrane; therefore, the average value of the intensity of the two points was taken as the fluorescence intensity of the GUV membrane. Typically, the fluorescence intensity of the rim of the GUV was measured every 10 s. For these analyses we used only GUVs with a diameter of 30−40 $\mu$m. To obtain the rate constant of CF-TP10 (or TP10)-induced pore formation ($k_P$), 3 independent experiments were carried out for each CF-TP10 or TP10 concentration using 20−30 single GUVs. Average values and standard errors of $k_P$ were calculated.

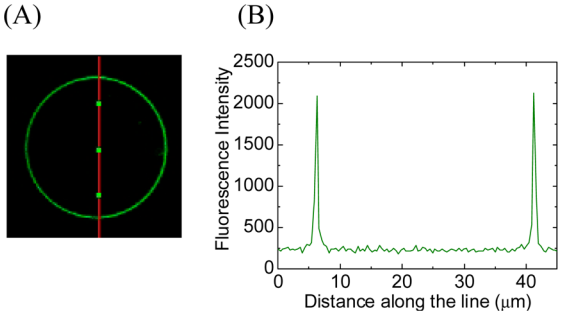


**Figure 1.** Measurement of the fluorescence intensity of the rim of a GUV (the GUV membrane) due to CF-TP10. A vertical line which goes through the center of the GUV was drawn for each GUV (A). The green circle corresponds to the GUV membrane and the red line corresponds to the vertical line. (B) shows a fluorescence intensity profile along the line. The two points with the highest intensity correspond to the GUV membrane. The average value of the intensity of these two points was taken as the fluorescence intensity of the GUV membrane.

## RESULTS AND DISCUSSION

**Translocation of CF-TP10 across the Lipid Membrane of GUVs before Pore Formation.** We first investigated the interaction of CF-TP10 with single 20%DOPG/79%DOPC/1%biotin-lipid-GUVs containing AF647 using CLSM. The interaction was carried out in buffer H containing 0.1 M glucose at 25 °C and was analyzed using the single GUV method. Figure 2A shows a typical result of the effect of the interaction of 1.9 $\mu$M CF-TP10 with single GUVs. The CF-TP10 solution was continuously provided to the GUV surroundings through a micropipet, so the equilibrium CF-TP10 concentration near the GUV was essentially the same as that in the micropipet.[17,21] A fluorescence microscope image of the GUV (Figure 2A (1)) shows a high concentration of AF647 inside the GUV. During the addition of the 1.9 $\mu$M solution of CF-TP10, the fluorescence intensity inside the GUV remained essentially constant over the first 212 s, after which the fluorescence intensity gradually decreased (Figure 2A (1) and red curve in Figure 2B). After 310 s, the fluorescence intensity was 30% of the initial intensity (at $t$ = 0), although a fluorescence microscope image of the same GUV due to CF-TP10 (Figure 2A (2)) shows that the GUV was intact and spherical. As discussed in our reports on magainin 2 and lysenin,[16−19] the decrease in fluorescence intensity results from the leakage of AF647 from the GUV through CF-TP10-induced pores in the membrane. Thus, the time at which the fluorescence intensity began to rapidly decrease ($t$ = 212 s) corresponds to the time when pores were formed in the membrane.

On the other hand, a fluorescence microscope image of the GUV due to the fluorescence of CF-TP10 (Figure 2A (2)) shows that the fluorescence intensity of the rim of the GUV (the GUV membrane) gradually increased, and that by about 125 s it is essentially saturated (green squares in Figure 2B). This is despite the fact that the fluorescence intensity of the aqueous solution outside the GUV was low. These observations indicate that CF-TP10 binds rapidly to the GUV membrane, and that the binding constant of CF-TP10 to the membrane is large.

The same experiments were carried out using 20 single GUVs. The gradual leakage of AF647 from a GUV started stochastically (Figure 2C), indicating that pores were formed stochastically. In all the examined GUVs, the fluorescence intensity of the GUV membrane became essentially saturated prior to pore formation. If we consider the irreversible two-state transition from the state of intact GUV (i.e., nonleaked GUV) to the state of GUV with pores (i.e., leaked GUV), we can obtain the rate constant of the two-state transition from the analysis of the time course of the fraction of intact GUVs, $P_{intact}(t)$, among the population of GUVs examined, from which the fluorescent probe did not leak over time $t$. Here we define this rate constant as the rate constant of peptide-induced pore formation in lipid membranes.[16−18] Figure 2D shows that the value of $P_{intact}$ of 20%DOPG/79%DOPC/1%biotin-lipid-GUVs decreased with time, and that the curve of the time course of $P_{intact}$ was fit well by the single exponential decay function defined by eq 1:

$$P_{intact}(t) = \exp\{-k_P(t - t_{eq})\} \quad (1)$$


dx.doi.org/10.1021/bi401406p | Biochemistry 2014, 53, 386−396

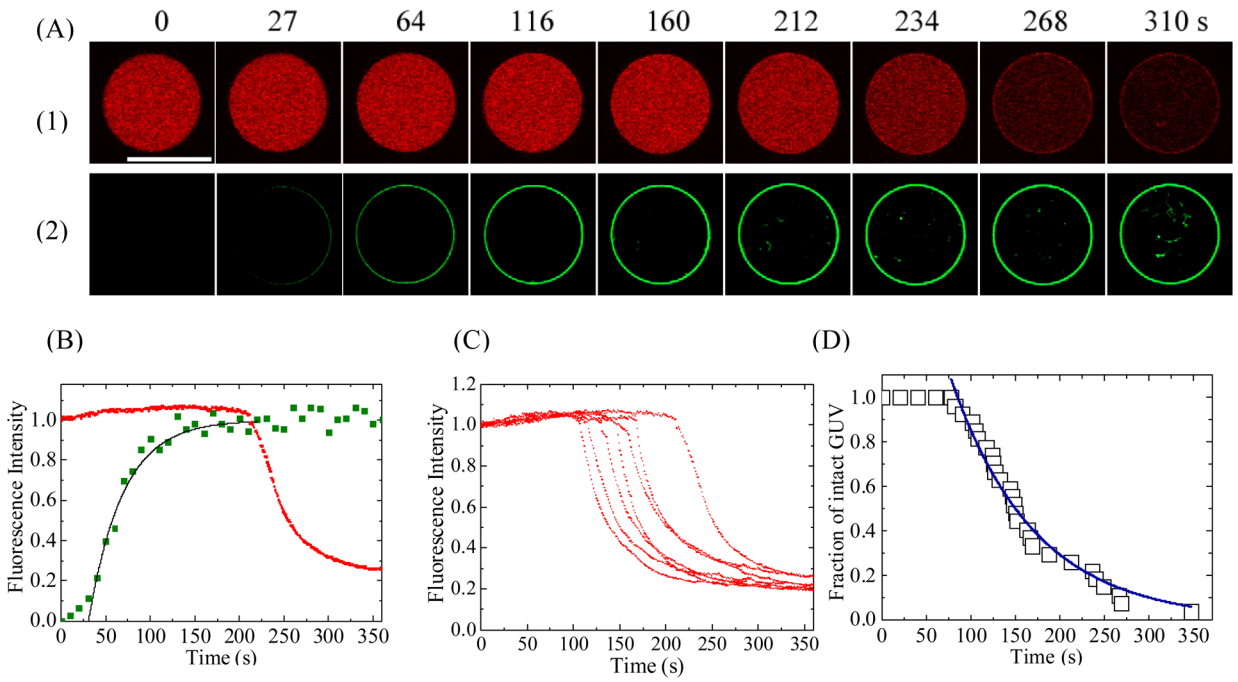


**Figure 2.** Leakage of AF647 and penetration of CF-TP10 in single 20%DOPG/79%DOPC/1% biotin-lipid-GUVs induced by 1.9 $\mu$M CF-TP10. (A) CLSM images of (1) AF647 and (2) CF-TP10. The numbers above each image show the time in seconds after CF-TP10 addition was started. The bar corresponds to 30 $\mu$m. (B) Time course of the change in normalized fluorescence intensity of the GUV shown in (A). Red and green points correspond to the fluorescence intensity of AF647 inside the GUV and of CF-TP10 in the rim of the GUV, respectively. The solid black line represents the best fit curve using eq 7. The obtained value of $k_{app}$ was 0.026 $s^{-1}$. (C) Other examples of the change in fluorescence intensity of AF647 inside single GUVs over time, using the same conditions as in (A). (D) Time course of $P_{intact}$ of 20%DOPG/79%DOPC/1%biotin-lipid-GUV. The solid blue line represents the best fit curve using eq 1. The obtained value of $k_p$ was 0.011 $s^{-1}$ and that of $t_{eq}$ was 85 s.

where $k_p$ is the rate constant of CF-TP10-induced pore formation and $t_{eq}$ is a fitting parameter denoting the time required for equilibrium binding of CF-TP10 to the GUV membrane. Three independent experiments similar to the experiment shown in Figure 2D were carried out to obtain the value for $k_p$. The average value of $k_p$ was then calculated using the results of all the independent experiments. The average value of $k_p$ for 1.9 $\mu$M CF-TP10 was 0.010 ± 0.001 $s^{-1}$, calculated from three independent experiments ($N$ = 3). We also investigated the rate constant of TP10-induced pore formation using the single GUV method and determined that it was 0.003 ± 0.001 $s^{-1}$ for 1.9 $\mu$M TP10 ($N$ = 3), which is smaller than the rate constant for CF-TP10. Figure 3 shows the dependence of the rate constant of CF-TP10 (or TP10)-induced pore formation on the concentration of CF-TP10 (or TP10), supporting the above result. The difference in rate constant is likely due to the binding constant of CF-TP10 with lipid membranes being larger than the binding constant of TP-10. Recently the same analysis using the time course of $P_{intact}$ of single GUVs was successfully applied to the external tension-induced pore formation in a GUV to obtain its rate constant.[25]

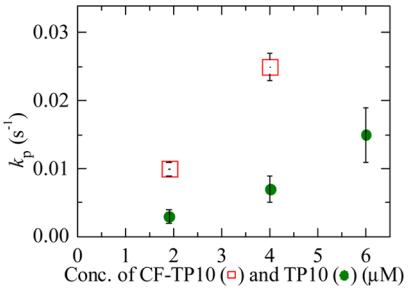


**Figure 3.** The dependence of the rate constant of CF-TP10 (or TP10)-induced pore formation in 20%DOPG/79%DOPC/1%biotin-lipid membranes on concentration. TP10 (green ●) and CF-TP10 (red □). The rate constant of CF-TP10-induced pore formation was obtained by the analysis of the leakage of AF647 and that of TP10-induced pore formation was obtained by the analysis of leakage of calcein. The average values and standard errors of $k_p$ were obtained.

To elucidate whether CF-TP10 enter the inside of a GUV under the experimental conditions of Figure 2, we used CLSM to investigate the interaction of CF-TP10 with single 20% DOPG/79%DOPC/1%biotin-lipid-GUVs containing smaller vesicles composed of 20%DOPG/80%DOPC and containing AF647. Figure 4A shows a typical experimental result of the effect of the interaction of 1.9 $\mu$M CF-TP10 with a single GUV. Figure 4A(1),B shows that CF-TP10 induced pores in the GUV membrane at 210 s, and then AF647 leaked through the pores rapidly. On the other hand, Figure 4A(2) shows that the fluorescence intensity of the GUV membrane gradually increased and at 100 s was almost saturated (green squares in Figure 4B). Some fluctuations of the intensity of the GUV membrane were caused by the smaller vesicles inside the GUV near the GUV membrane. At the beginning of the interaction, there was no fluorescence inside the GUV, but after 140 s, fluorescence intensity was observed due to the membranes of the smaller vesicles inside the GUV ($t$ = 144, 167, and 194 s in Figure 4A(2)). This fluorescence occurred before CF-TP10-induced pore formation (210 s). These results indicate that CF-TP10 entered the inside of the GUV from the outside by translocating across the GUV membrane and then bound to the membrane of the smaller vesicles inside the GUV. The entry of CF-TP10 into the inside of the GUV occurred before pore


dx.doi.org/10.1021/bi401406p | *Biochemistry* 2014, 53, 386−396

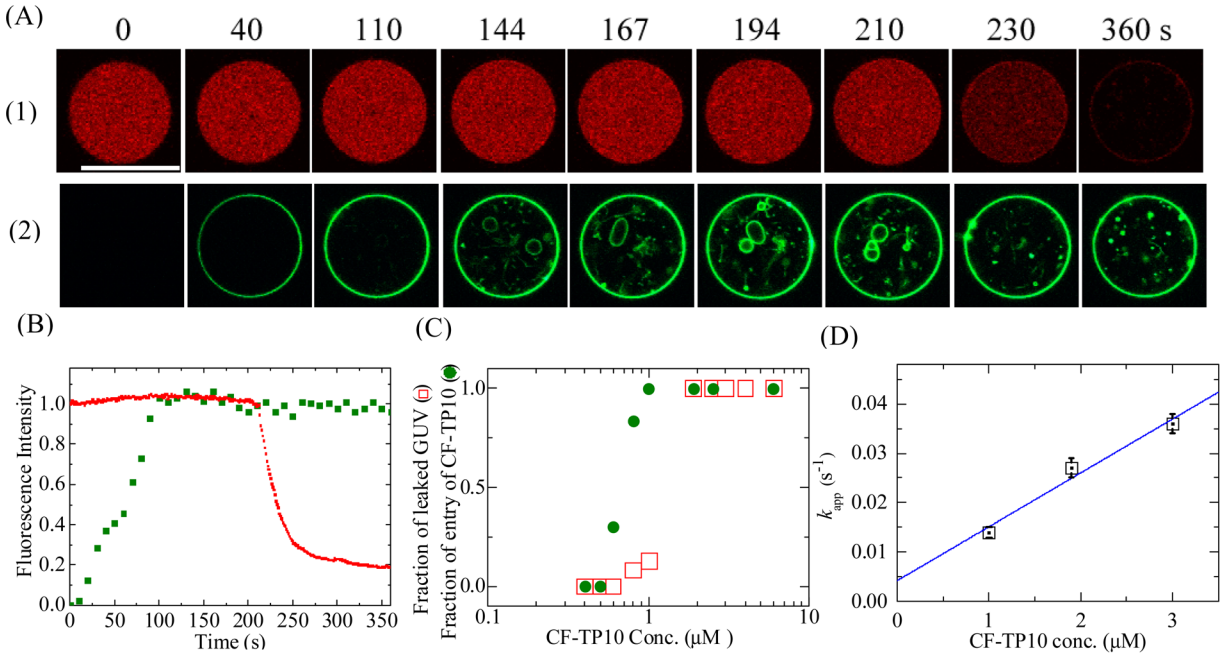


**Figure 4.** Leakage of AF647 and entry of CF-TP10 into single 20%DOPG/79%DOPC/1%biotin-lipid-GUVs containing smaller vesicles, induced by 1.9 $\mu$M CF-TP10. (A) CLSM images of (1) AF647 and (2) CF-TP10. The numbers above each image show the time in seconds after CF-TP10 addition was started. The bar corresponds to 30 $\mu$m. (B) Time course of the change in normalized fluorescence intensity of the GUV shown in (A). Red and green points correspond to the fluorescence intensity of AF647 inside the GUV and of CF-TP10 in the rim of the GUV, respectively. (C) Dependence of the fraction of entry of CF-TP10 before pore formation on the concentration of CF-TP10 (green ●). For comparison, the dependence of the fraction of leaked GUV after 6 min interaction on the concentration of CF-TP10 is shown (red □). (D) Dependence of $k_{app}$ on CF-TP10 concentration. The time course of the change in the fluorescence intensity of 15−25 GUVs with a diameter of 30−40 $\mu$m was measured. The average values and standard errors of $k_{app}$ were obtained. The solid blue line represents the best fit curve using eq 8.

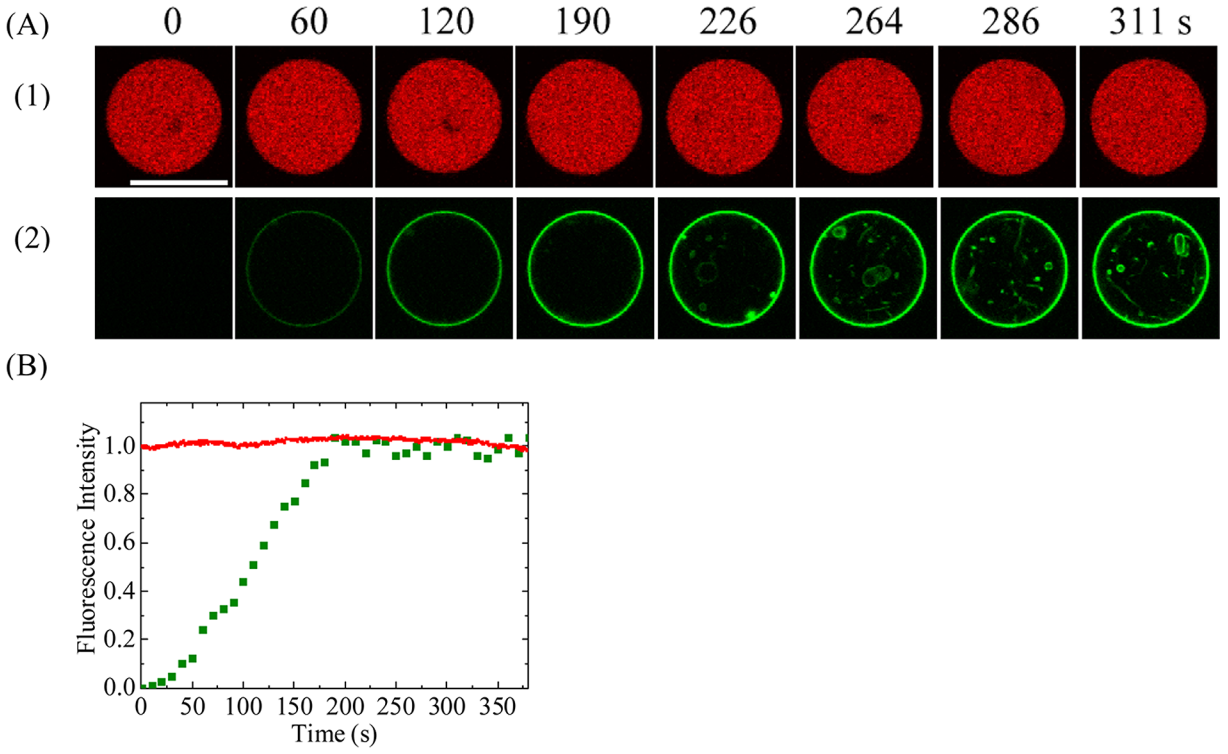


**Figure 5.** Leakage of AF647 and entry of CF-TP10 into single 20%DOPG/79%DOPC/1%biotin-lipid-GUVs containing smaller vesicles, induced by 1.0 $\mu$M CF-TP10. (A) CLSM images of (1) AF647 and (2) CF-TP10. The numbers above each image show the time in seconds after CF-TP10 addition was started. The bar corresponds to 30 $\mu$m. (B) Time course of the change in normalized fluorescence intensity of the GUV shown in (A). Red and green points correspond to the fluorescence intensity of AF647 inside the GUV and of CF-TP10 in the rim of the GUV, respectively.


dx.doi.org/10.1021/bi401406p | *Biochemistry* 2014, 53, 386−396

formation. Next, we investigated the concentration dependence of the entry of CF-TP10 into a GUV before pore formation (i.e., before the leakage of AF647). Figure 5 shows the interaction of 1.0 $\mu$M CF-TP10 with single 20%DOPG/79% DOPC/1%biotin-lipid-GUVs containing smaller vesicles and AF647. The data indicate that CF-TP10 entered the inside of the GUV, although pore formation did not occur before 6 min. At a CF-TP10 concentration of ≤1.0 $\mu$M, the probability of pore formation at 6 min was low (less than 0.2; Figure 4C), supporting the conclusion that CF-TP10 entered the intact GUV by translocating across the GUV membrane without pore formation. In the case of 0.8 $\mu$M CF-TP10, of the 12 GUVs examined, entry of CF-TP10 occurred before pore formation in 10 (i.e., fraction of entry of CF-TP10 = 0.83). Figure 4C shows the concentration dependence of the fraction of entry of CF-TP10. At and above 0.6 $\mu$M CF-TP10, the entry of CF-TP10 was observed in some examined GUVs, and the fraction of entry of CF-TP10 increased with an increase in CF-TP10 concentration and became 1.0 at and above 1.0 $\mu$M. These results clearly indicate that the translocation of CF-TP10 is a necessary condition, but not a sufficient condition, for the pore formation, i.e., some other factor determines the pore formation (see the detailed discussion later).

We next considered the kinetics of entry of CF-TP10 and the time course of CF-TP10 concentration in the GUV membrane, $C_M(t)$ [M]. In the single GUV method, in the system considered there are only a single GUV and its surrounding aqueous solution at first. Then we add continuously a given concentration of CF-TP10 solution to the neighborhood of the single GUV by a micropipet until the end of observation of the GUV. Thereby, the CF-TP10 concentration in aqueous solution near the GUV increased from zero to a constant equilibrium value, $C_{out}^{eq}$[M], for a short time, and then it was held constant during the interaction of CF-TP10 with the single GUV, which was almost the same as that of the solution in the micropipet.[17,21] This situation is almost the same as that of the surface plasmon resonance analysis,[26] but very different from that of the LUV suspension method where the peptide concentration in aqueous solution changes with time and greatly depends on lipid concentration. At the first step of the interaction, CF-TP10 binds at the membrane interface of the outer monolayer of the GUV. Since this surface area is limited, we can assume that there is the maximum concentration of the binding site of CF-TP10 at the membrane interface of the monolayer, i.e., $C_M^{max}$[M]. It is noted that $C_M^{max}$ also has a physical meaning of the maximum concentration of the binding site of CF-TP10 at the membrane interface of the bilayer. Here we consider that one CF-TP10 molecule binds with one binding site, and thereby the CF-TP10 concentration in the monolayer is the same as the concentration of the occupied binding site of CF-TP10 at the membrane interface, and thereby $C_M^{max}$ is the maximum concentration of CF-TP10 in the monolayer and also in the bilayer. We further assume that the Langmuir binding isotherm holds here. $\theta_{OM}$ and $\theta_{IM}$ are the fraction of binding sites occupied by CF-TP10 in the outer and inner monolayer, respectively. Hence, the CF-TP10 concentration in the outer monolayer, $C_{OM}$ [M], is $\theta_{OM}C_M^{max}$, and the CF-TP10 concentration in the inner monolayer, $C_{IM}$[M], is $\theta_{IM}C_M^{max}$. The rate of the binding of CF-TP10 with the outer monolayer of the GUV from aqueous solution is proportional to the concentration of unoccupied binding sites, $(1-\theta_{OM})C_M^{max}$, and the CF-TP 10 concentration in the aqueous solution outside the GUV, $C_{out}^{eq}$. Thus, the rate is equal to $k_{ON}C_{out}^{eq}(1-\theta_{OM})C_M^{max}$, where $k_{ON}$ is the rate constant of the binding. Next, the transfer of CF-TP10 from the outer to the inner monolayer occurs at a rate constant $k_{FF}$. Finally, CF-TP10 transfers from the inner monolayer of the GUV into the aqueous solution inside the GUV at a rate constant of $k_{OFF}$. We also have to consider backward reactions. Thereby, $C_{OM}$, $C_{IM}$, and the CF-TP10 concentration in the aqueous solution inside the GUV, $C_{in}$, can be expressed by the following differential equations:

$$\frac{dC_{OM}}{dt} = k_{ON}C_{out}^{eq}(1-\theta_{OM})C_M^{max} - k_{FF}\theta_{OM}C_M^{max} + k_{FF}\theta_{IM}C_M^{max} - k_{OFF}\theta_{OM}C_M^{max} \quad (2)$$

$$\frac{dC_{IM}}{dt} = k_{FF}\theta_{OM}C_M^{max} - k_{FF}\theta_{IM}C_M^{max} - k_{OFF}\theta_{IM}C_M^{max} + k_{ON}C_{in}(1-\theta_{IM})C_M^{max} \quad (3)$$

$$\frac{dC_{in}}{dt} = k_{OFF}\theta_{IM}C_M^{max} - k_{ON}C_{in}(1-\theta_{IM})C_M^{max} \quad (4)$$

Initially, $C_{in}$ is very low and so the term $k_{ON}C_{in}(1-\theta_{IM})C_M^{max}$ can be neglected. We can obtain the time derivative of the average concentration of CF-TP10 in the GUV bilayer, $C_M$, using eqs 2, 3, and $C_M = (C_{OM} + C_{IM})/2$.

$$\frac{dC_M}{dt} = \frac{1}{2}\{k_{ON}C_{out}^{eq}(1-\theta_{OM})C_M^{max} - k_{OFF}\theta_{OM}C_M^{max} - k_{OFF}\theta_{IM}C_M^{max}\}$$
$$= \frac{1}{2}\{k_{ON}C_{out}^{eq}C_M^{max} - k_{ON}C_{out}^{eq}C_{OM} - k_{OFF}C_{OM} - k_{OFF}C_{IM}\} \quad (5)$$

Generally it is difficult to obtain $C_M(t)$ due to some unknown parameters. If the transfer of CF-TP10 between the outer and inner monolayers is fast, i.e., the rate of the transfer is larger than that of the binding of CF-TP10 and that of its transfer from the membrane to aqueous solution (i.e., $k_{FF} \gg k_{ON}C_{out}^{eq}$, and $k_{FF} \gg k_{OFF}$), we can approximate that $C_{OM} \approx C_{IM} \approx C_M$. Under this condition, eq 5 can be converted to eq 6:

$$\frac{dC_M}{dt} = \frac{1}{2}k_{ON}C_{out}^{eq}C_M^{max} - \left(\frac{1}{2}k_{ON}C_{out}^{eq} + k_{OFF}\right)C_M \quad (6)$$

The solution of this differential eq 6 under the initial condition ($C_M(0) = 0$) becomes

$$C_M(t) = \frac{C_M^{max}}{1 + \frac{1}{2K_BC_{out}^{eq}}}\left[1 - \exp\left\{-\left(\frac{1}{2}k_{ON}C_{out}^{eq} + k_{OFF}\right)t\right\}\right] = A[1 - \exp(-k_{app}t)] \quad (7)$$

where

$$k_{app} = k_{ON}C_{out}^{eq}/2 + k_{OFF} \quad (8)$$

where $K_B = k_{ON}/k_{OFF}$ is the binding constant of CF-TP10 to the lipid membrane and $k_{app}$ is the apparent rate constant of the increase in CF-TP10 concentration in the GUV membrane, $C_M(t)$. The time course of the fluorescence intensity of the rim of the GUV (Figure 2B) was fit well by eq 7 (the black line in Figure 2B), which gave a value for the rate constant $k_{app}$ of 0.026 $s^{-1}$. We also obtained the dependence of $k_{app}$ on CF-


dx.doi.org/10.1021/bi401406p | Biochemistry 2014, 53, 386−396

TP10 concentration. As expected from eq 8, $k_{app}$ increased linearly with an increase in CF-TP10 concentration, $C_{out}^{eq}$. Fitting the data to eq 8 in Figure 4D provided values for $k_{ON}$ and $k_{OFF}$: $k_{ON} = 2.2 \times 10^4$ $M^{-1}$ $s^{-1}$ and $k_{OFF} = 4.2 \times 10^{-3}$ $s^{-1}$ (i.e., $K_B = 5.2 \times 10^6$ $M^{-1}$). Since CF-TP10 contains a hydrophobic fluorescent probe, CF, $K_B$ of CF-TP10 may be larger than that of TP10. However, we do not have other experimental evidence that the transfer of CF-TP10 between outer and inner monolayers is fast, and hence we need further studies.

We also investigated the interaction of CF-TP10 with single DOPC-GUVs containing AF647 and smaller vesicles inside the GUVs using CLSM. We obtained essentially identical results as for 20%DOPG/79%DOPC/1%biotin-lipid-GUVs, although a lower concentration of CF-TP10 induced leakage of AF647 and translocation of CF-TP10 across the lipid membrane into single GUVs prior to pore formation.

The above results indicate that CF-TP10 can transfer from the outer to the inner monolayer before pore formation. The concentration imbalance of CF-TP10 between the outer and the inner monolayer induces strain in the lipid membrane, which may be one of the factors of the transfer.[10] Such transfer of CF-TP10 would perturb the structure of lipid membranes, which might induce a transient leakage of small molecules such as ions. Molecular dynamics simulations indicate that some amphipathic peptides can transfer from the outer to the inner monolayer.[27,28] However, the mechanism of this transfer is not completely clear from the biophysical point of view at present, and thereby further studies are indispensable.

**Size of TP10-Induced Pores in the Lipid Membranes of GUVs.** In order to examine the size of the TP10-induced pores in lipid membranes, we investigated the leakage of a water-soluble fluorescent probe, TRD-40k, using phase contrast fluorescence microscopy. The molecular weight distribution of TRD-40k is 35 000−50 000 according to the manufacturer, and its Stokes−Einstein radius, $R_{SE}$, is 5.0 nm.[18] Figure 6A shows the effect of the interaction of 6 $\mu$M TP10 with single 20% DOPG/79%DOPC/1%biotin-lipid-GUVs containing TRD-40k. Prior to TP10 addition, a phase contrast microscope image of the GUV showed high contrast (Figure 6A-1) due to the difference in the concentration of sucrose and glucose between the inside (0.1 M sucrose) and the outside (0.1 M glucose) of the GUV. A fluorescence microscope image of the same GUV (Figure 6A-2) showed a high concentration of TRD-40k inside the GUV at this time. During addition of a 6 $\mu$M solution of TP10, the fluorescence intensity inside the GUV remained similar over the first 52 s, followed by a gradual decrease in fluorescence intensity (Figure 6A-2,C). After 360 s, less than 10% of the original fluorescence intensity was detected inside the GUV. The time course of this decrease in fluorescence intensity of the inside of the GUVs due to TRD-40k was fit well by a single exponential decay curve (Figure 6C). A comparison of the phase contrast images in Figure 6A-1 and A-3 also shows a substantial loss in the phase contrast of the GUV, indicating that leakage of TRD-40k was accompanied by passage of sucrose and glucose through the same pore. The images also show that the diameter of the GUV decreased by 16%, and the presence of a few small, high-contrast particles on the membrane of the GUV. These data indicate that TRD-40k can pass through TP10-induced pores in the GUV membrane. When the same experiments were carried out using 25 single GUV, similar leakage of TRD-40k from a GUV started stochastically. Figure 6E shows that the value of

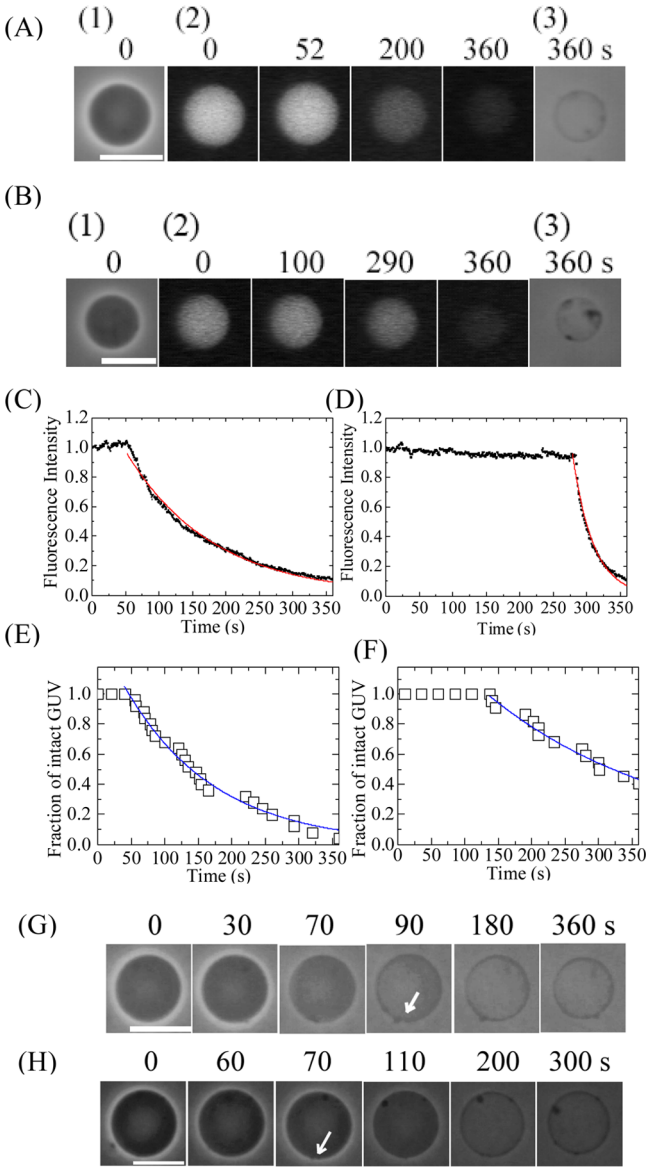


**Figure 6.** The size of TP10-induced pores in 20%DOPG/79%DOPC/1%biotin-lipid-GUVs. (A,C) Leakage of TRD-40k from single 20% DOPG/79%DOPC/1%biotin-lipid-GUVs induced by 6 $\mu$M TP10 in buffer H at 25 °C. (A) Fluorescence images (2) show that the TRD-40k concentration inside the GUV progressively decreased after the addition of TP10. The numbers above each image show the time in seconds after TP10 addition was started. Also shown are phase contrast images of the GUV at time 0 (1) and 360 s (3). The bar corresponds to 20 $\mu$m. (C) Time course of the change in the normalized fluorescence intensity of the GUV shown in (A). The solid red line represents the best fit curve using a single exponential decay function. (B,D) Leakage of TRD-10k from single 20%DOPG/79% DOPC/1%biotin-lipid-GUVs induced by 4 $\mu$M TP10 in buffer H at 25 °C. (B) Fluorescence images (2) show that the TRD-10k concentration inside the GUV progressively decreased after the addition of TP10. The numbers above each image show the time in seconds after TP10 addition was started. Also shown are phase contrast images of the GUV at time 0 (1) and 360 s (3). The bar corresponds to 20 $\mu$m. (D) Time course of the change in the normalized fluorescence intensity of the GUV shown in (B). The solid red line represents the best fit curve using a single exponential decay function. (E) Time course of $P_{intact}$ of 20%DOPG/79%DOPC/1% biotin-lipid-GUV containing TRD-40k in the presence of 6 $\mu$M TP10 in buffer H at 25 °C. The solid blue line represents the best fit curve using eq 1. The obtained value of $k_P$ was 0.008 $s^{-1}$. (F) Time course of


dx.doi.org/10.1021/bi401406p | Biochemistry 2014, 53, 386−396

**Figure** 6. continued

$P_{intact}$ of 20%DOPG/79%DOPC/1%biotin-lipid-GUV containing TRD-10k in the presence of 4 $\mu$M TP10 in buffer H at 25 °C. The solid blue line represents the best fit curve using eq 1. The obtained value of $k_p$ was 0.004 $s^{-1}$. (G) Leakage of sucrose from single 20%DOPG/79%DOPC/1%biotin-lipid-GUVs induced by 6 $\mu$M TP10. Phase contrast images are shown. A white arrow shows a local rupture of the membrane. The bar corresponds to 20 $\mu$m. (H) Leakage of sucrose from single 20% DOPG/79%DOPC/1%biotin-lipid-GUVs containing TRD-40k induced by 6 $\mu$M TP10. Phase contrast images are shown. A white arrow shows a local rupture of the membrane. The bar corresponds to 20 $\mu$m.

$P_{intact}$ of 20%DOPG/79%DOPC/1%biotin-lipid-GUVs containing TRD-40k decreased with time, and that the curve of the time course of $P_{intact}$ was fit well by the single exponential decay function defined by eq 1. The average value of $k_p$ for 6.0 $\mu$M TP10 was 0.010 ± 0.001 $s^{-1}$ and the average value of $t_{eq}$ was 53 ± 13 s, calculated from four independent experiments similar to Figure 6E ($N$ = 4). This $k_p$ value is a little smaller than that obtained using 20%DOPG/79%DOPC/1%biotin-lipid-GUVs containing calcein. In 50% of the GUVs examined, the diameter of the GUV did not change, but in the other 50% the diameter decreased by 10−20%. In some GUVs, the multistep of the decrease in the fluorescence intensity of the GUV was observed. Similar results were obtained for the TP10-induced leakage of TRD-10k (Figure 6B,D,F). The average value of $k_p$ for 4.0 $\mu$M TP10 was 0.005 ± 0.001 $s^{-1}$ and the average value of $t_{eq}$ was 190 ± 40 s ($N$ = 3). At present we do not know the reason the rate constants of the TP10-induced pore formation in the GUVs containing TRD-40k are a little smaller than those in the GUVs containing calcein. There may be some interactions between TP10 and TRD-40k inside the GUVs.

To understand the mechanism underlying the decrease in GUV diameter, the interaction of TP10 with single 20% DOPG/79%DOPC/1%biotin-lipid-GUVs containing 0.1 M sucrose and no TRD-40k was investigated using phase contrast microscopy. Figure 6G shows that after single-site rupture of the GUV membrane (shown by a white arrow), the GUV diameter gradually decreased. However, the local rupture did not always decrease the diameter of GUVs. Similar results were obtained for the interaction of TP10 with single 20%DOPG/79%DOPC/1%biotin-lipid-GUVs containing TRD-40k (Figure 6H). On the basis of these results, large molecules such as TRD-40k and TRD-10k can permeate through a TP10-induced pore or the TP10-induced local rupture of the membrane. The mechanism of the TP10-induced rupture of the membrane and the resultant decrease in diameter of the GUV remains unknown, although a similar decrease in the diameter of a GUV was observed in the interaction of mastoparan with a GUV.[29]

On occasion, a smaller vesicle inside a GUV exited through the TP10-induced pore or the local rupture. Figure 7 shows an example of the exit of a smaller vesicle with a diameter of 1−2 $\mu$m from the mother GUV in the interaction of 2.5 $\mu$M CF-TP10 with a 20%DOPG/79%DOPC/1%biotin-lipid-GUV. At 97.6 s, a few small vesicles were observed near the membrane inside the mother GUV, and from 98.8 to 99.9 s they have exited the mother GUV.

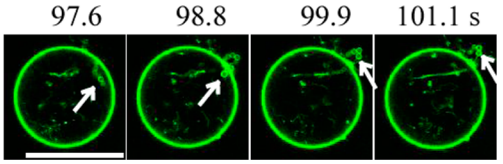


**Figure 7.** Exit of small vesicles with a diameter of 1−2 $\mu$m from the inside of a GUV induced by 2.5 $\mu$M CF-TP10. Experimental conditions are the same as for Figure 2. A white arrow shows smaller vesicles which exited from the mother GUV. The bar corresponds to 40 $\mu$m.

The results clearly show that large molecules such as TRD-40k and vesicles with a diameter of 1−2 $\mu$m can translocate across the lipid bilayer. This is the first direct experimental evidence that TP10 can deliver large cargo through lipid membranes. The mechanism of these TP10-induced pore formation and local rupture is not clear at present.

**Translocation of Peptides Across Lipid Membrane and Peptide-Induced Pore Formation.** As shown in the kinetics of the concentration of CF-TP10 in the GUV membrane, the translocation of CF-TP10 across the lipid membranes (i.e., the transfer of CF-TP10 from the outer to the inner monolayer) occurs continuously, indicating that the activation energy of the translocation is low. In contrast, CF-TP10 (or TP10) induced pore formation in lipid membranes stochastically, indicating that the activation energy of the pore formation is large. Moreover, the results in the report clearly indicate that CF-TP10 translocates across the lipid membranes at an early stage, and then in a subsequent stage, pore formation occurs in the lipid membranes (i.e., pore formation occurs after the translocation of peptides). At low concentrations of CF-TP10 (from 0.6 to 1 $\mu$M) the translocation of CF-TP10 did not induce pore formation in most GUVs (Figure 4C). These results indicate that the translocation of CF-TP10 is a necessary condition, but not a sufficient condition, for pore formation, i.e., some other factor determines pore formation. The translocation of CF-TP10 increases the concentration of CF-TP10 in the inner monolayer, and the kinetic analysis suggests that the concentrations of CF-TP10 in both monolayers are similar. The $C_M^{max}$value increases with an increase in CF-TP10 concentration in a buffer, and thereby we can reasonably consider that the CF-TP10 concentration in both monolayers plays an important role in pore formation. This characteristic is similar to that of the pore formation induced by melittin, a bee venom peptide with a lytic activity against eukaryote cells.[30] It is important to note that pore formation took a long time after the CF-TP10 concentration in the membrane became a maximum, steady value, $C_M^{max}$ (e.g., Figure 2B and Figure 4B), which is different from the case of melittin.

In contrast, as for antimicrobial peptide, magainin 2, we have proposed the different scheme of pore formation as follows. Magainin 2 molecules locate in the membrane interface of only the outer monolayer before pore formation, which induces a stretching of the inner monolayer. We consider that this stretching plays an important role in pore formation. The data of the magainin 2-induced leakage of TRD-10k and TRD-40k from single GUVs show the transient, rapid leakage in the initial stage followed by a stage of slow leakage, indicating that magainin 2 molecules initially induce a transient, large pore in lipid membranes following which the radius of the pore decreases to a stable smaller size.[18] It is also reported that the


dx.doi.org/10.1021/bi401406p | *Biochemistry* 2014, 53, 386−396

α5 segment from the proapoptotic protein Bax (Baxα5) induced pores in lipid membranes and the size of this pore is large at the initial stage and then decreased to a smaller, equilibrium size with time.[31] As shown in Figure 6, most of the time courses of TP10-induced leakage of TRD-10k and TRD-40k from single GUVs were fit well by single exponential decay curves, indicating that the size of the TP10-induced pore does not change with time. This result is different from that of magainin 2 and Baxα5 peptides. To confirm our hypothesis on the magainin 2-induced pore, we need the experimental evidence of the location of magainin 2 in a single GUV before pore formation, which can be obtained using the same method in this report.

**Advantage of the Single GUV Method.** We succeed in obtaining new information on the interaction of TP10 with lipid membranes using the single GUV method. We separated the elementary processes of TP10-induced leakage of fluorescent probe (i.e., TP10-induced pore formation in lipid membranes and leakage of fluorescent probe through the pores), and succeed in determining the rate constant of TP10-induced pore formation. We obtained the time course of the CF-TP10 concentration in the membrane, and its relationship with the entry of CF-TP10 into the inside of GUVs. The simultaneous experiment of the leakage of the fluorescent probe and the entry of CF-TP10 clearly shows that CF-TP10 translocates across the lipid membrane before pore formation. These results cannot be obtained using the LUV suspension method.

After we had submitted this manuscript, a paper on the translocation of cationic amphipathic peptides across the GUV membrane was published.[32] The experimental method used in their paper (here we call it the GUV suspension method) is different from the single GUV method used in this report; in the GUV suspension method many GUVs were suspended in a solution of a water-soluble fluorescent probe, carboxyfluorescein (CF), and Lissamine Rhodamine B (Rh) labeled peptides (TP10W and DL1a). The GUVs contained smaller inner GUVs. First, CF and peptides entered the inside of the outer GUV, and then the translocation of peptides into the inside of the inner GUVs and influx of CF into the inner GUVs occurred. The authors observed that the translocation of peptide into the inner GUVs occurred gradually and the influx of CF into the inner GUVs rapidly. However, in their paper there are no quantitative results such as peptide concentration dependence of the translocation of peptides and the rate constant of the peptide-induced pore formation. The rate of the translocation of peptides across the inner GUV membrane in their paper (characteristic time is 10 min) was very low compared with that of CF-TP10 in our report, although it is difficult to compare the rates because the equilibrium concentration of peptide is unknown in their paper. Irrespective of these differences in the experimental data and method, their results support the conclusion in this report qualitatively.

The advantage of the single GUV method over their GUV suspension method is as follows. (1) In the single GUV method, we can control the concentration of peptides outside a single GUV (i.e., $C_{out}^{eq}$), and thereby we can obtain detailed information on peptide concentration dependence of the translocation of peptides and the peptide-induced pore formation (e.g., Figure 3, Figure 4C and D). In contrast, in the GUV suspension method, many GUVs are added in a given concentration of peptide solution, and hence the peptide concentration outside the GUV depends on GUV concentration (i.e., lipid concentration) in the suspension, which cannot be controlled well, and it also changes with time because the binding of peptides with GUV membranes and the entry of peptides into the inside of the GUVs increase with time. This is the same situation as the LUV suspension method. On the other hand, in the single GUV method, we cannot determine the peptide to lipid molar ratio in the system, which is determined in the LUV suspension method and the GUV suspension method. (2) In the single GUV method it is easier to carry out many experiments using a single GUV and analyze these results statistically to obtain the rate constants of the elementary steps. (3) In the single GUV method, we can follow rapid reaction of peptide translocation and pore formation because we can observe the GUV from the start of the interaction of peptides with the GUV (i.e., $t = 0$). On the other hand, the advantage of the GUV suspension method is that no special apparatus and experimental technique such as handling of micropipet are required. However, it is evident that both the single GUV method and the GUV suspension method are superior to the LUV suspension method, and hence these methods will become powerful tools to reveal the interaction of peptides such as CPPs with lipid membranes.

From the results in this report, we should learn an important lesson for investigation of translocation of peptides such as CPPs across the lipid membranes. Some peptides such as TP10 and magainin 2[18] induce a pore whose size is larger than that of the peptide. In this case, after the pore formation peptides can easily enter the vesicles by diffusion through the pore, and thereby the increase in peptide concentration inside the GUV or at the membranes of smaller vesicles inside the GUV does not indicate translocation of peptide across the membrane. Only when the transfer of peptides into the inside of GUVs occurs before pore formation, or the size of the peptide-induced pore is smaller than that of the peptide, does the increase in the peptide concentration inside the GUV correspond to the translocation of peptide across the membrane. Thereby to study the translocation of peptides, the simultaneous measurement of peptide-induced pore formation and the transfer of peptides into the inside of GUVs is indispensable.[33]

**Biological Implications.** In this report we clearly show that TP10 translocates across the lipid membranes and subsequently the pore formation occurs in the membrane. The size of the pore is so large that TRD-40K and vesicles with a diameter of 1−2 μm can pass through the pore. This provides experimental evidence to explain why TP10 can deliver large cargo through plasma membranes without the need for special transport mechanisms such as those found in cells. Based on the results in this report, we can reasonably consider that if TP10 could dissociate from its cargo at or near the plasma membranes the yield of cellular uptake of cargo would increase because the translocation of TP10 is expected to be faster than that of TP10 connected with a hydrophilic cargo such as oligonucleotide and protein. The experimental results of TP10-induced cellular uptake of decoy oligonucleotide targeting the Myc protein may support the above hypothesis; the yield of cellular uptake of a noncovalent electrostatic complex of TP10 with Myc decoy (i.e., the TP10-Myc decoy complex) is much larger than that of a complex of TP10 which is covalently attached with peptide nucleic acid with TP10.[9] However, we do not know whether a complex of TP10 covalently attached to proteins and oligonucleotides can induce pore formation and translocate across lipid membranes. To validate our hypothesis and address the above question, it is important to investigate effects of cargo

molecules and the kinds of attachment of cargo with TP10 on the TP10-induced translocation of cargo molecule across lipid membranes.

## CONCLUSION

The results in this report show that CF-TP10 translocated continuously across the lipid membrane of a single GUV before pore formation (i.e., without leakage of fluorescent probes), and then subsequently, pore formation occurred in lipid membranes. Moreover, at a lower concentration of CF-TP10, pore formation did not occur after the translocation of CF-TP10, indicating that some other factor is necessary for pore formation. We measured the time course of CF-TP10 concentration at the GUV membrane, which was fit well by a theoretical equation based on a model for CF-TP10 translocation across the GUV membrane. After the translocation of CF-TP10 was complete, the pores were formed in the GUV membranes stochastically. We determined the rate constant of CF-TP10-induced pore formation, which increased with an increase in CF-TP10 concentration. These results clearly show that translocation of CF-TP10 into the GUVs and CF-TP10-induced pore formation are different phenomena, and that the former occurs in the absence of the latter. We also investigated the size of the TP10-induced pore in lipid membranes and found that large molecules such as TRD-40K, and vesicles with a diameter of 1−2 $\mu$m, translocate across the lipid bilayer. This result indicates that large molecules can pass through the TP10-induced pores in lipid membranes. As discussed in the Introduction, TP and TP10 can deliver a large protein such as an antibody, oligonucleotide, and colloidal gold (diameter 10 nm) as cargo,[7,9] but the mechanism is poorly understood. Our results directly indicate that TP10 can deliver large proteins and gold particles as cargo through the TP10-induced pores in the lipid membrane without the need for special mechanisms found in cells. In conclusion, the results in this report reveal the elementary steps of entry of TP10 into a single vesicle and TP10-induced pore formation in the membrane, and the new experimental methods in this report will be used to reveal the mechanism of these phenomena and to design new CPPs and antimicrobial peptides.

## AUTHOR INFORMATION

### Corresponding Author

*Tel/Fax: 81-54-238-4741. E-mail: spmyama@ipc.shizuoka.ac.jp

### Funding

This work was supported in part by a Grant-in-Aid for Scientific Research (B) (No. 21310080 in 2009−2012) from the Japan Society for the Promotion of Science (JSPS), and also by a Grant-in-Aid for Scientific Research in Priority Areas (System Cell Engineering by Multiscale Manipulation) (No. 18048020 in 2006−2008, and No. 20034023 in 2008−2010) from the Ministry of Education, Culture, Sports, Science and Technology (MEXT) of Japan to M.Y.

### Notes

The authors declare no competing financial interest.

## ACKNOWLEDGMENTS

This work was partially carried out using instruments at the Center for Instrumental Analysis, Shizuoka University.

## REFERENCES

(1) Lindgren, M., Hällbrink, M., Prochiantz, A., and Langel, Ű. (2000) Cell-penetrating peptides. *Trends Pharmacol. Sci. 21*, 99−103.
(2) Magzoub, M., and Gräslund, A. (2004) Cell-penetrating peptides: small from inception to application. *Q. Rev. Biophys. 37*, 147−195.
(3) Zorko, M., and Langel, Ű. (2005) Cell-penetrating peptides: mechanism and kinetics of cargo delivery. *Adv. Drug Delivery Rev. 57*, 529−545.
(4) Madani, F., Lindberg, S., Langel, Ű., Futaki, S., and Gräslund, A. (2011) Mechanisms of cellular uptake of cell-penetrating peptides. *J. Biophys. 414729*, 10 pages.
(5) Korenm, E., and Torchilin, V. P. (2012) Cell-penetrating peptides: breaking through to the other side. *Trends Mol. Med. 18*, 385−393.
(6) Pooga, M., Hällbrink, M., Zorko, M., and Langel, Ű. (1998) Cell penetration by transportan. *FASEB J. 12*, 67−77.
(7) Pooga, M., Kut, C., Kihlmark, M., Hällbrink, M., Fernaeus, S., Raid, R., Land, T., Hallberg, E., Bartfai, T. M., and Langel, Ű. (2001) Cellular translocation of proteins by transportan. *FASEB J. 15*, 1451−1453.
(8) Soomets, U., Lindgren, M., Gallet, X., Pooga, M., Hällbrink, M., Elmquist, A., Balaspiri, L., Zorko, M., Pooga, M., Brasseur, R., and Langel, Ű. (2000) Deletion analogues of transportan. *Biochim. Biophys. Acta 1467*, 165−176.
(9) E.L.−Andaloussi, S., Johansson, H., Magnusdottir, A., Järver, P., Lundberg, P., and Langel, Ű. (2005) TP10, a delivery vector for decoy oligonucleotides targeting the Myc protein. *J. Controlled Release 110*, 189−201.
(10) Yandek, L. E., Pokomy, A., Floren, A., Knoeike, K., Langel, Ű., and Almeida, P. F. F. (2007) Mechanism of the cell-penetrating peptide transportan 10 permeation of lipid bilayers. *Biophys. J. 92*, 2434−2444.
(11) Yandek, L. E., Pokomy, A., and Almeida, P. F. F. (2008) Small changes in the primary structure of transportan 10 alter the thermodynamics and kinetics of its interaction with phospholipid vesicles. *Biochemistry 47*, 3051−3060.
(12) Barany-Wallje, E., Gaur, J., Lundberg, P., Langle, Ű., and Gräslund, A. (2007) Differential membrane perturbation caused by the cell penetrating peptide TP10 depending on attached cargo. *FEBS Lett. 581*, 2389−2393.
(13) Yamazaki, M. (2008) The single GUV method to reveal elementary processes of leakage of internal contents from liposomes induced by antimicrobial substances. *Advances in Planar Lipid Bilayers and Liposomes 7*, 121−142.
(14) Saitoh, A., Takiguchi, K., Tanaka, Y., and Hotani, H. (1998) Opening-up of liposomal membranes by talin. *Proc. Natl. Acad. Sci. U.S.A. 95*, 1026−1031.
(15) Baumgart, T., Hess, S. T., and Webb, W. W. (2003) Imaging coexisting fluid domains in biomembrane models coupling curvature and line tension. *Nature 425*, 821−824.
(16) Tamba, Y., and Yamazaki, M. (2005) Single giant unilamellar vesicle method reveals effect of antimicrobial peptide, magainin-2, on membrane permeability. *Biochemistry 44*, 15823−15833.
(17) Tamba, Y., and Yamazaki, M. (2009) Magainin 2-induce pore formation in the lipid membranes depends of its concentration in the membrane interface. *J. Phys. Chem. B 113*, 4846−4852.
(18) Tamba, Y., Ariyama, H., Levadny, V., and Yamazaki, M. (2010) Kinetic pathway of antimicrobial peptide magainin 2-induced pore formation in lipid membranes. *J. Phys. Chem. B 114*, 12018−12026.
(19) Alam, J. M., Kobayashi, T., and Yamazaki, M. (2012) Single giant unilamellar vesicle method reveals lysenin-induced pore formation in lipid membranes containing sphingomyelin. *Biochemistry 51*, 5160−5172.
(20) Tamba, Y., Ohba, S., Kubota, M., Yoshioka, H., Yoshioka, H., and Yamazaki, M. (2007) Single GUV method reveals interaction of Tea catechin (-)-epigallocatechin gallate with lipid membranes. *Biophys. J. 92*, 3178−3194.
(21) Tanaka, T., Sano, R., Yamashita, Y., and Yamazaki, M. (2004) Shape changes and vesicle fission of giant unilamellar vesicles of liquid-

ordered phase membrane induced by lysophosphatidylcholine. *Langmuir 20*, 9526−9534.
(22) Thorén, P. E. G., Persson, D., Karlsson, M., and Nordén, B. (2000) The Antennapedia peptide penetratin translocates across lipid bilayers-the first direct observation. *FEBS Lett. 482*, 265−268.
(23) Tamba, Y., Terashima, H., and Yamazaki, M. (2011) A membrane filtering method for the purification of giant unilamellar vesicles. *Chem. Phys. Lipids 164*, 351−358.
(24) Stamou, D., Duschl, C., Delamarche, E., and Vogel, H. (2003) Self-assembled microarray of attolitter molecular vesicle. *Angew. Chem. 115*, 5738−57451.
(25) Levadny, V., Tsuboi, T., Belaya, M., and Yamazaki, M. (2013) Rate constant of tension-induced pore formation in lipid membranes. *Langmuir 29*, 3848−3852.
(26) Gaidukov, L., Fish, A., and Mor, A. (2003) Analysis of membrane-binding properties of dermaseptin analogues: relationships between binding and cytotoxicity. *Biochemistry 42*, 12866−12874.
(27) Lopez, C. F., Nielsen, S. O., Srinivas, G., DeGrado, W. F., and Klein, M. L. (2006) Probing membrane insertion activity of antimicrobial polymers via coarse-grain molecular dynamics. *J. Chem. Theory Comput. 2*, 649−655.
(28) Leontiadou, H., Mark, A. E., and Marrink, S. J. (2006) Antimicrobial peptides in action. *J. Am. Chem. Soc. 128*, 12156−12161.
(29) Dos Santos Cabrera, M. P., Alvares, D. S., Leite, N. B., de Souza, B. M., Palma, M. S., Riske, K. A., and Neto, J. R. (2011) New insight into the mechanism of action of wasp mastoparan peptides: lytic activity and clustering observed with giant vesicles. *Langmuir 27*, 10805−10813.
(30) Lee, M.-T., Sun, T.-L., Hung, W.-C., and Huang, H. W. (2013) Process of inducing pores in membranes by melittin. *Proc. Natl. Acad. Sci. U.S.A. 110*, 14243−14248.
(31) Fuertes, G., Garcia-Sáez, A., Esteban-Martin, S., Giménez, D., Sánchez-Muñoz, O. L., Schwille, P., and Salgado, J. (2010) Pores formed by Bax$\alpha$5 relax to a smaller size and keep at equilibrium. *Biophys. J. 99*, 2917−2925.
(32) Wheaten, S. A., Ablan, F. D. O., Spaller, B. L., Trieu, J. M., and Almeida, P. F. (2013) Translocation of cationic amphipathic peptides across the membranes of pure phospholipid giant vesicles. *J. Am. Chem. Soc. 135*, 16517−16525.
(33) Boll, A., Jatho, A., Czudnochowski, N., Geyer, M., and Steinem, C. (2011) Mechanistic insights into the translocation of full length HIV-1 Tat across lipid membranes. *Biochim. Biophys. Acta 1808*, 2685−2693.